UNIVERSITÀ DEL PIEMONTE ORIENTALE

SCUOLA DI MEDICINA

Dipartimento di Scienze della Salute

Master Degree in Medical Biotechnology

Role of DGKA and DGKZ in THP-1 osteoclastogenesis

Relatore:

Prof. Gianluca Baldanzi

Firmato digitalmente da Gianluca Baldanzi
Data: 30.06.2026 18:08:57 CEST
Organizzazione: UNIVERSITA' DEGLI STUDI DEL PIEMONTE ORIENTALE/01943490027

Elaborato finale di:

Biazzo Giorgio

N. Matricola: 20043665

Anno accademico 2025/2026

Table of contents

Abstract

Osteoclasts are bone-resorbing cells whose activation and differentiation are controlled by M-CSF and RANKL, which regulate osteoclast-specific genes such as TRAP and Cathepsin K. Diacylglycerol kinases (DGKs) are lipid-metabolizing enzymes that phosphorylate diacylglycerol (DAG) to generate phosphatidic acid (PA), and are implicated in macrophage and osteoclast regulation. In DGKα knockout mice, DGKα was shown to act as a regulator of macrophage activation, with knockout macrophages displaying increased cell cycling, migration, and wound-site influx (Manigat et al., 2021). DGKζ knockout mice were found to be osteoporotic, with a marked increase in osteoclast number, and bone marrow macrophages from these mice formed more numerous, larger, and highly resorptive osteoclasts in vitro (Zamani et al., 2015). On this basis, we hypothesized that DGKα and DGKζ knockout could alter osteoclastogenesis. Human Protein Atlas and FANTOM/CAGE data identified DGKZ as the most highly expressed DGK isoform in THP-1 cells, monocytes, and macrophages, followed by DGKA, DGKG, DGKD, DGKE, and DGKQ. QRT-PCR performed on THP-1 cells during their differentiation into macrophages and osteoclasts showed DGKE and DGKG downregulation during osteoclastogenesis, while the remaining isoforms showed stable or non-significant trends. Concordance between database and experimental data was observed for DGKA, DGKG, DGKH, DGKQ, and DGKZ, with partial agreement for DGKI and discrepancies for the remaining isoforms. THP-1 cells were then edited by CRISPR-Cas9 to knockout DGKα or DGKζ, and subjected to differentiation with PMA for macrophage commitment and M-CSF plus RANKL for osteoclastogenesis, over 8 to 10 days. Knockout efficiency was confirmed by western blotting, showing an 87% reduction in DGKα and a 91% reduction in DGKζ protein levels. Compared to control cells, which underwent the expected phenotypic transition and generated large multinucleated syncytia, both DGKα KO and DGKζ KO cells displayed increased cellular debris, reduced spreading, and an overall inability to reach the same morphological complexity. The increase in cell diameter observed during differentiation was pronounced in control cells, but much less pronounced in both knockout lines, with the final osteoclast population remaining significantly smaller. Moreover, both DGKα KO and DGKζ KO osteoclasts displayed significantly fewer nuclei per cell, supporting the idea that both isoforms are functionally involved in fusion-related events controlling fully developed osteoclast-like syncytia. TRAP expression was higher in DGKα KO and DGKζ KO cells than in controls, despite their failure to achieve comparable morphological complexity. This pattern suggests that loss of DGKα and DGKζ does not abolish the initial response to differentiation stimuli, but specifically compromises later stages associated with cytoplasmic expansion and fusion. The discrepancy with existing literature, where DGKζ loss in primary murine precursors increased osteoclast formation, likely reflects that the two models capture different stages of osteoclastogenesis: in primary murine cells DGKζ loss may act early to expand the precursor pool, whereas in THP-1 monoculture it predominantly impairs late morphological maturation, resulting in defective spreading and fusion despite preserved transcriptional markers. Overall, these findings indicate that DGKα and DGKζ are required for osteoclast-like morphological differentiation in THP-1 cells, even though their loss produces context-dependent outcomes across different experimental systems.

Introduction

The present work starts from data collected from the scientific literature indicating that the DGKs play relevant roles in macrophage and osteoclast regulation and function. In this context, we hypothesized that DGKα and DGKζ knockout may alter osteoclastogenesis. In this study after consulting databases regarding the presence of DGKs in monocytes, macrophages and THP-1 cell line, we decided to knockout DGKα and DGKζ on THP-1 cells. These cells were differentiated with PMA followed by M-CSF and RANKL administration, shifting from monocyte to macrophage and osteoclast stages. Morphological changes, together with TRAP evaluation were studied, to further understand the role of DGKα and DGKζ in THP-1 osteoclastogenesis.

1. Osteoclasts and molecular pathways

Osteoclasts are large multinucleated cells that play a central role in bone homeostasis by resorbing damaged bone and promoting bone repair via signaling cross-talk with bone stromal cells specifically resident osteocytes and bone-forming osteoblasts (Diepenhorst et al., 2017). Osteoclast differentiation and function is kept under tight regulation, osteocytes are capable of orchestrating biochemical signals to maintain bone homeostasis by locally secreting osteoclastogenic factors. The coupling between osteoclasts and osteoblasts is called *bone remodeling* and requires a balance between the processes of bone resorption and formation, preventing accumulation of microdamages (Pereira et al., 2018). Osteoclasts derive from the haematopoietic lineage following fusion and differentiation of mononucleated monocytes from the blood and bone marrow (Diepenhorst et al., 2017). HSCs give rise to common myeloid progenitors (CMPs), which differentiate into granulocyte/macrophage progenitors (GMPs) mediated by stimulation with granulocyte/macrophage stimulating factor (GM-CSF). GMPs further differentiate into monocytes/macrophage lineage to become osteoclast progenitors, which enter the blood circulation and migrate towards bone surfaces where they fuse and finally become multinucleated osteoclasts (Omi & Mishina, 2022). Osteoprogenitors are commonly found in the bone marrow, and they are known to express two of the most important cytokines needed for osteoclast formation: macrophage colony-stimulating factor (M-CSF) and receptor activator of nuclear factor-κB ligand (RANKL) (Søe et al., 2021).

Particularly, M-CSF stimulation of myeloid cells expressing the corresponding receptor, CSF1R (also called c-Fms), supports osteoclast progenitors' survival and induces the expression of RANK (Ono & Nakashima, 2018). Moreover, M-CSF exists in both membrane-bound and secreted forms and is expressed by osteoblasts and stromal cells (Mun et al., 2020). CSF1R expression in immature myeloid precursors is low, while it increases progressively during myeloid maturation. M-CSF/CSF1R signaling highly supports osteoclast precursor proliferation and induces RANK expression; it also regulates osteoclast motility and cytoskeletal reorganization in a c-Src-dependent manner. Indeed, studies showed that CSF1R-deficient mice displayed severe osteoclast deficiency together with defective bone architecture (Mun et al., 2020).

Concerning RANKL, its binding to RANK activates NF-kB and MAPK pathways, resulting in the induction of two key osteoclastic transcription factors, c-Fos and nuclear factor-activated T cells c1 (NFATc1). Activation of these factors regulates osteoclast specific genes, such as tartrate-resistant acid phosphatase (TRAP) and CathepsinK, required for osteoclast differentiation (Omi & Mishina, 2022).

RANKL binding to RANK induces the trimerization of RANK and the recruitment of an adaptor protein, TRAF6, via three TRAF6-binding sites in its C-terminal cytoplasmic tail. TRAF6 is the major adaptor protein responsible for mediating signaling cascades that are activated by RANKL, and activated TRAF6 stimulates NF-κB activity by activating activator protein AP-1 (Park et al., 2017). NFATc1 is a master transcription factor for osteoclastogenesis, and it is found downstream of NF-κB and MAPK signaling, then c-Fos and Jun proteins dimerize to form AP-1, and together NF-κB, AP-1, NFATc2, ATF4 and Jdp2 are recruited to the promoter region of the NFATc1 gene after RANKL stimulation, together inducing NFATc1 (Ono & Nakashima, 2018).

After the initial induction of NFATc1 by NF-κB, c-Fos/AP-1, and NFATc2, RANK signaling functions together with the activation of immunoglobulin-like receptor/immunoreceptor tyrosine-based activation motif (ITAM) signaling, which leads to the robust amplification of NFATc1 and its translocation to the nucleus, where it binds with DNA in combination with other transcription factors to upregulate the transcription of NFATc1 target genes. The negative regulators are downregulated during osteoclast differentiation in response to RANK : MafB, IRF-8 and Bcl6 usually repress NFATc1

expression. These three factors are downregulated by the transcription repressor B-lymphocyte-induced maturation protein 1 (Blimp1), which is induced by RANKL stimulation during osteoclastogenesis (Park et al., 2017).

1.1 Osteoclast fusion and bone resorption

Once pre-osteoclasts arrive to the bone, they must penetrate through the cell layers covering resting bone surfaces, the bone marrow envelope, and bone lining cells. These pre-osteoclasts secrete a variety of matrix metalloproteases (MMPs), such as MMP9 and MMP14, shown to selectively cleave collagen fibres. Once the layer of collagen underneath bone lining cells has been removed, a migrating pre-osteoclast will get in contact with the mineralized bone surface, and together they will fuse to become a multinucleated osteoclast (Søe et al., 2021).

A cell–cell fusion regulator, DC-STAMP is a seven-helix transmembrane protein and has been isolated from dendritic cells, IL-4-induced macrophages, and osteoclasts. DC-STAMP is specifically required for osteoclast cell–cell fusion and it is a bone-remodeling factor regulating both osteoclasts and osteoblasts. Osteoclast cell–cell fusion is considered essential for re-organization of the cytoskeleton and thus critical for osteoclast function (Miyamoto, 2011).

Osteoclastic bone resorption is achieved by the dissolution of hydroxyapatite by secretion of acids, followed by the degradation of the bone matrix organic component trough proteolysis (Omi & Mishina, 2022). The formation of actin rings by podosomes, the "sealing zone", and the "ruffled border", maintains local acidification and accumulation of matrix-degrading enzymes between the cell and bone surface. (Pereira et al., 2018). The resorption compartment is formed by the attachment of osteoclasts to the bone surface through the sealing zone. Inside the sealed zone, H^+, Cl^-, CtsK and MMP-9 are secreted to demineralize and degrade the collagen I-rich matrix (Ono & Nakashima, 2018)(Park et al., 2017). Osteoclasts resorb bone in two different ways: the intermittent and stationary resorption mode resulting in rounded cavities called *pits*, and the continuous resorption mode where the osteoclast moves during resorption resulting in deep elongated cavities called *trenches* (Omi & Mishina, 2022).

1.2 TRAP and CathepsinK

Osteoclasts are generally characterised by two criteria: the presence of multinucleation, with a number of nuclei >3 and TRAP activity (Diepenhorst et al., 2017). Once activated osteoclasts express TRAP, encoded by the ACP5 gene, involved in hydrolysis of bone matrix activity and in the dephosphorylation of specifc protein substrates (osteopontin) (Ethiraj et al., 2022). The phosphatase activity of TRAP forms the basis of its histological detection and TRAP staining intensity increases with multinucleation of osteoclasts.(Ethiraj et al., 2022) (Pereira et al., 2018).

CathepsinK is a papain-like cysteine protease member of the cathepsin family of lysosomal proteases (Drake et al., 2017). As a protease, CathepsinK is the primary enzyme responsible for degradation of type I collagen, which composes 90% of the bone organic matrix (Drake et al., 2017). The expression of CTSK is also the most present among the known cathepsins in osteoclasts (Ono & Nakashima, 2018). Within osteoclasts, CTSK has been shown to reside in lysosomes, cytoplasmic vesicles, and along the osteoclast–bone resorptive interface before its release into the resorptive lacunae. CathepsinK expression is mediated by RANKL-induced activation of the transcription factor NFATc1, which targets the CTSK promoter. (Drake et al., 2017)

2. Diacylglycerol kinases

Diacylglycerol kinases (DGKs) are lipid-metabolizing enzymes that phosphorylate diacylglycerol (DAG) to generate phosphatidic acid (PA), functioning in both intracellular signaling cascades and membrane lipid homeostasis. DGKs modulate cellular processes through two primary mechanisms: by consuming DAG to suppress DAG-mediated signaling pathways such as protein kinase C (PKC) and Ras-GRP; and by producing PA to activate downstream cascades involving mTOR, Raf, and phosphodiesterases (PDEs) (Liu et al., 2025). Both DAG and PA can act as important second messengers and DGKs act as metabolic integrators, coordinating responses related to growth, proliferation, immune activation and metabolic reprogramming (Liu et al., 2025)(Sim et al., 2020).

DAG and PA respectively play different roles in endocytic events like vesicular trafficking, secretory pathway regulation, and Golgi apparatus function. DAG regulates

membrane trafficking activating PKC, PKD, and downstream signaling cascades; it is involved in phosphatidylinositol regulation and subsequent Ca^{2+} influx. Local concentration of PA regulates trafficking, since PA-enriched membranes exhibit increased negative curvature, lowering the energetic barrier for membrane fission. Moreover, it serves as a docking site for the recruitment of specific proteins. (Xie et al., 2015)

2.1 DGK isoforms, structure and localization

There are ten DGK isozymes (α, β, γ, δ, ε, ζ, η, θ, ι, and κ) that have been described in mammals, but the presence of different splicing isoform, such as ζ1 and ζ2, expands the width of this family (Racca et al., 2025) (Sakane et al., 2020).

Class I DGKs (DGKA, DGKB and DGKG) possess two calcium-binding EF-hand motifs and a recoverin homology domain, making them responsive to intracellular Ca^{2+} fluctuations and capable of transducing DAG-mediated signals (Liu et al., 2025). Class II DGKs (DGKD, DGKH and DGKK) contain a phosphoinositide-binding PH domain and, except for DGKK, a C-terminal sterile alpha motif involved in protein–protein interactions. Class III DGKE is the most structurally minimal isoform, characterized by two C1 domains, a catalytic domain, and an ER-targeting transmembrane region that confers membrane localization and selectivity for polyunsaturated fatty acid-containing substrates (Liu et al., 2025). Class IV DGKs (DGKZ and DGKI) are enriched in protein–protein interaction domains, including ankyrin repeats, a MARCKS-related domain, and a PDZ domain, which mediates anchoring of membrane receptors to the cytoskeleton (Lee & Zheng, 2010)(Gravina et al., 2023). Lastly, Class V DGKQ contains three atypical C1 domains, a PH domain, and a proline/glycine-rich region that likely functions as a docking site for SH3 domain-containing proteins; notably, its PH domain includes a Ras-association motif suggesting potential interactions with RhoA and links to small GTPase signaling (Sim et al., 2020).

DGKs display highly specific expression patterns, and most cells co-express multiple isoforms, often belonging to different subfamilies, indicating non-redundant and specialized functions (Baldanzi & Malerba, 2019). In addition, DGKs can translocate to distinct subcellular compartments depending on receptor stimulation, supporting the

concept that their activity is spatially restricted to specific DAG pools generated upon cellular activation (Fazio et al., 2020).

Most of the isoforms are partially associated with the plasma membrane. This localization can be constitutive, as observed for DGKκ, or induced by stimulation with specific agonists. For example, DGKδ1 translocates to the plasma membrane upon phorbol ester exposure, DGKα following T cell receptor engagement, and DGKθ and DGKζ in response to activation of certain G protein-coupled receptors (Fazio et al., 2020). In addition, several isoforms are found in the nucleus, where inositide signaling regulates cell cycle progression and differentiation and is involved in pathological conditions including cancer and myelodysplastic syndromes. Nuclear DAG can be generated independently from cytoplasmic pools, for example in response to IGF-1 or thrombin, and its levels fluctuate independently during the cell cycle (Fazio et al., 2020). Several DGK isoforms, including DGKα, ζ, and ι, shuttle between the nucleus and cytoplasm, DGKγ translocates into the nucleus, DGKθ accumulates in nuclear speckles and DGKα is mainly localized at the nuclear periphery (Fazio et al., 2020). Isoform-specific regulation is further influenced by structural motifs. DGKα, DGKβ, and DGKγ contain EF-hand domains sensing intracellular Ca^{2+}, triggering conformational changes that promote translocation to DAG-rich membranes and activation of enzymatic activity (Liu et al., 2025). DGKδ is mainly localized at the endoplasmic reticulum, Golgi and endosomes, whereas DGKη is primarily associated with endosomes but can be recruited to the plasma membrane upon signaling events (Fazio et al., 2020)(Xie et al., 2015). DGKε is uniquely characterized by strong substrate specificity for 1-stearoyl-2-arachidonoyl-sn-glycerol and a stable ER membrane association due to its transmembrane domain (Nakano et al., 2016). DGKζ is predominantly cytosolic at rest but redistributes upon stimulation to the nucleus, plasma membrane, and cytoskeleton, where its localization is regulated mainly by its MARCKS homology domain and PDZ-binding motif (Zamani et al., 2015). DGKθ translocates from the cytosol to the plasma membrane following PKC or GPCR activation (Fazio et al., 2020). Several studies have also demonstrated DGK association with cytoskeletal components, suggesting a relevant role in cytoskeletal remodeling and cell morphology. DGKs interact with proteins involved in cytoskeletal regulation, including Rac, Rho GTPases, PIP5K, Cdc42, and Rho-GDI. DGKζ forms complexes with Rac1, Rho-GDI, and PAK1, DGKβ co-localizes

with actin filaments, and DGKζ has been detected at the leading edge of C2 myoblasts and glioblastoma cells, where it co-purifies with cytoskeletal proteins (Fazio et al., 2020).

With the increasing recognition of DGKs as key modulators of lipid signaling, inflammation, and cellular metabolism, therapeutic targeting of DGK isoforms has attracted growing interest across fields such as oncology, immunotherapy, and metabolic diseases (Liu et al., 2025). Currently, there are some clinical trials involving DGKα or DGKζ, assessing their pharmacological properties and efficacy for their use as anticancer agents (Racca et al., 2025). These compounds aim to rebalance aberrant DAG–PA signaling by either restoring DAG-mediated immune activation or suppressing oncogenic PA-dependent pathways (Liu et al., 2025)

DGKα is the best-characterized oncogenic isoform, promoting tumor proliferation, angiogenesis, and survival through pathways such as PKCζ–NF-κB in melanoma, Raf–MEK–ERK in hepatocellular carcinoma (HCC), PDE4A1–mTOR in glioblastoma, and cyclin D3 (CCND3) in lung cancer. Additionally, DGKα facilitates migration in bladder cancer and predicts recurrence in intrahepatic cholangiocarcinoma. It also promotes angiogenesis via HIF-1α activation and reduces ROS accumulation by inhibiting NOX4 through PA generation (Liu et al., 2025). More recent work in acute myeloid leukemia has also highlighted DGKα and DGKζ as key determinants of leukemic cell viability and as potential therapeutic vulnerabilities (Gorla et al., 2025).

2.2 DGKs in macrophages and osteoclasts

Macrophages are important effector cells of the innate immune system and perform many varied and context-dependent functions. They are among the first cells to respond in the event of injury and also are necessary for tissue remodeling and repair (Manigat et al., 2021). Macrophages are highly plastic cells, sensitive to their microenvironment, with the ability to polarize to an M1 pro-inflammatory phenotype in response to LPS and/or IFNγ, and to an M2 anti-inflammatory phenotype in response to IL-4 and tissue damage (Mahajan et al., 2020).

In Dgkζ deficient mice it is observed a defective macrophage polarization to an M1 pro-inflammatory phenotype, arguing that Dgkζ deletion induces macrophage hypo-responsiveness to TLR signaling and limits M1 macrophage activation, thus highlighting

the importance of Dgkζ in DAG/PA axis in autoimmune and inflammatory diseases driven by macrophages (Mahajan et al., 2020). Other studies described that LPS induced proinflammatory cytokine production is decreased in DGKζ deficient bone marrow macrophages, demonstrating that DGKζ signaling regulates macrophage function (Okada et al., 2012). Subsequently other findings described novel roles for DGKα and DGKγ. In DGKα knockout mice DGKα acted as a regulator of macrophage activation, increasing their responsiveness. In particular the wound healing process was altered in DGKα deficient mice, and using a burn model, the wounds were smaller and showed an increase in the number of local macrophages. An in vitro model explained an increased cell cycling and migration of DGKα knockout macrophages, suggesting that an increased proliferation or influx of these macrophages can explain their higher numbers at wound sites (Manigat et al., 2021). While DGKγ can negatively regulates macrophage differentiation through its catalytic action operating on the cytoskeleton. In particular DGKγ may act affecting gene expression of important proteins such as adhesion molecules and lysosomal enzymes. In this paper, the results showed that DGKγ can act as a negative regulator at early stages of the phorbol ester-induced signal transduction cascade resulting in macrophage differentiation of leukemia cells (HL-60 and U937 cells) (Yamada et al., 2003).

Multinucleated foreign body giant cells (FBGCs) are formed through monocyte-derived macrophage fusion (McNally & Anderson, 2003). In a macrophage cell line (RAW264.7) the DGKδ inhibitor 4-hexylresorcinol (4HR) limited significantly the formation of multinucleated body giant cells (Kweon et al., 2014). While R59022, a DGKα inhibitor, prevented IL-4-induced multinucleated body giant cells formation and severely restricted cytoplasmic spreading (McNally & Anderson, 2003).

DAG-related pathways are also involved in bone remodeling. For instance, M-CSF, induces the generation of DAG, necessary for c-Fos expression, a transcription factor involved in osteoclast differentiation. (Zamani et al., 2015). These findings suggest that DAG may be a significant regulator of bone mass, controlling osteoclast formation by modulating c-Fos expression and affecting the osteoclast precursor proliferation via the β-catenin/cyclin D1 axis (Yang et al., 2017).

DGKs may participate in this complex scenario by regulating osteoclastogenesis, being the different isoenzymes, like DGKζ, highly expressed in macrophages and osteoclasts. For example in case of DGKζ deficiency, DAG accumulates and the osteoclastogenesis increases consistent with c-Fos rise. (Racca et al., 2025). Moreover, DGKζ knockout mice are osteoporotic due to a marked increase in osteoclast number, while in vitro DGKζ knockout bone marrow macrophages (BMMs) form more numerous, larger and highly resorptive osteoclasts. Interestingly, while increased DAG levels do not alter RANK/RANKL osteoclastogenic pathway, DGKζ deficiency increases responsiveness to the proliferative and pro-survival cytokine M-CSF (Zamani et al., 2015).

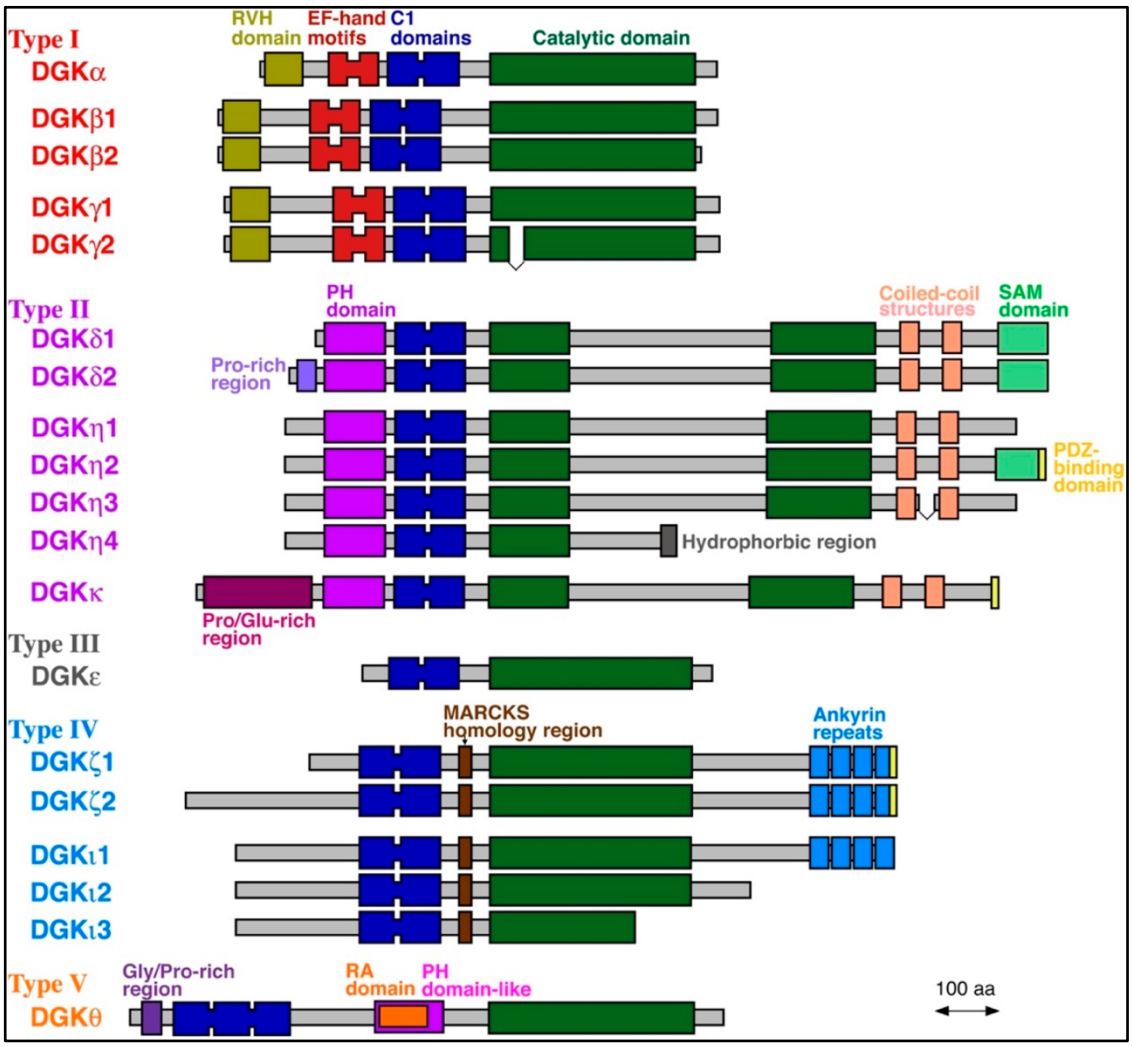

Fig. 1: *Mammalian DGK family* (Sakane et al., 2020).

3. THP-1 cell line

THP-1 is a human acute monocytic leukemia cell line isolated from the peripheral blood of a child with monocytic leukemia. Since its establishment in 1980, THP-1 has been widely used in research on macrophage-related signaling pathways and drug delivery studies (Liu et al., 2023). THP1 cells are globular suspended monocytes and under the stimulation of PMA, they are able to differentiate into adherent macrophages with a round or fusiform morphology (Li et al., 2017). PMA is the most commonly used inducer for THP-1 cell differentiation that can bind and activate protein kinases, activate transcription factors such as NF-κB, and promote the expression of macrophages associated proteins (Liu et al., 2023). The THP-1 cell line represent a simplified and reliable model to study monocyte and macrophage functions and responses, macrophage differentiation and possible effects from external stimuli in the surrounding environment (Chanput et al., 2014)(Forrester et al., 2018).

Monocytes and macrophages belong to the innate immune compartment, in which their major roles are recognition of foreign pathogens such as bacteria, proliferation to increase the amount of cells that are able to eliminate pathogens, production of pro-inflammatory and anti-inflammatory chemokines and cytokines, and phagocytosis. (Chanput et al., 2014). THP-1 cells can be stimulated using LPS and IFNγ to generate pro-inflammatory macrophages (M1) or using IL-4 and IL-13 or IL-10 to generate anti-inflammatory macrophages (M2) (Mohd Yasin et al., 2022). There are multiple advantages for the use of THP-1 cell line over PBMC-derived monocytes or macrophages. Their growing rate is higher compared to PBMC-derived monocytes, and they are safer to use due to the absence of infectious viruses or toxic products. THP-1 cells are an immortalized cell line that can be cultured in vitro for about three months without changes of cell sensitivity and activity. On the other hand PBMC-derived monocytes require inflammatory mediators like IL-1β, TNF-α or LPS to prevent apoptosis. The availability of PBMC-derived monocytes is often limited and these cells cannot be stored in liquid nitrogen. They also lack the homogeneous genetic background of THP-1, because high variation from individual donors is a common problem for the application of PBMC derived monocytes (Chanput et al., 2014). PMA concentration and incubation time are important to achieve proper THP-1 cells activation, which is associated with profound transcriptional

reprogramming (Liu et al., 2023). Using too low concentration of PMA will lead to insufficient differentiation, whereas too high concentration of PMA has toxic effects on cells. Liu et al. demonstrated that PMA concentrations lower than 200ng/ml showed no effect on the proliferative activity of THP-1 cells while concentration of 80ng/ml had a better induction effect. After the addition of PMA for 24h, the proportion of THP-1 cells with morphological changes was the largest, and then the cells gradually turned to round shape gradually decreasing in number (Liu et al., 2023). Suspended THP-1 cells without stimulation exhibited an adherence rate of 0% while the adherence rates of THP-1 cells following stimulation with 100 ng/ml PMA for 1, 2 and 3 days were 70.1, 94.3 and 97.1% respectively (Li et al., 2017).

THP-1 cells can also be inducted towards osteoclast differentiation. Once that THP-1 cells have been differentiated into macrophages, they can be further differentiated into osteoclasts using cytokines and exogenous hormones, such as M-CSF and RANKL (Wang and Shen, 2019). Li et al., demonstrated that the administration of 50 ng/ml M-CSF and 50 ng/ml RANKL was successfully able to induce osteoclast differentiation in macrophages. M-CSF is able to upregulate the expression of RANK, while RANKL facilitates the formation of TRAP-positive osteoclasts. As demonstrated in bone resorption assay, following 12 days of stimulation, high-dose PMA treatment exhibited the formation of TRAP-positive osteoclasts. Interestingly, the use of a two-step method is required to obtain mature osteoclasts, since PMA alone, or M-CSF with RANKL alone, do not induce the formation of osteoclasts. In the end, THP-1 cells are a reliable model to properly investigate osteoclast function, formation and key features (Li et al., 2017).

4. CRISPR-Cas9

Recently developed clustered regularly interspaced short palindromic repeats CRISPR-Cas technology its rapidly evolving in the gene therapy field, making a truly flexible tool for the treatment of human genetic diseases (Zhang, 2021). Recent discoveries have shown that bacteria have evolved a defense system that uses a series of small non-coding RNA molecules. The core of this defense mechanism, known as the CRISPR system, consists of genes that are organized in groups with repetitive sequences. First, when bacteria and archaea are infected by viruses, they respond by integrating into their genome short fragments of the viral DNA, called spacer DNA. These fragments produce small

non-coding RNAs, called crRNAs, which subsequently bind to a Cas protein encoded by a gene adjacent to the CRISPR sequence. In a sense, the CRISPR system is similar, in principle, to the process of immunization by a vaccine, with the “memory” of the past viral infection then used to progress from one exposure to protection from future exposures. The second phase of the CRISPR system consists of using this stored viral DNA sequence to find and destroy viral DNA molecules before they can harm the cell. The key to CRISPR immunity is an enzyme called nuclease Cas9. Guided by its crRNA, this enzyme recognizes small regions of the viral genome that match the RNA that it is carrying. In the second passage, the CRISPR locus is transcribed to produce a long RNA molecule, then processed in smaller crRNA, about 30 nucleotides long. In the third passage, the crRNA in complex with Cas proteins explores the cell in search of viral DNA, using complementarity to direct the destruction with of certain nucleases (Alberts et al., 2016).

The exportation of the CRISPR system from bacteria to practically any other experimental organism constitutes a revolutionary breakthrough in genetic engineering (Alberts et al., 2016). In summary, the simplicity and high efficiency of the CRISPR/Cas9 system allows affordable genome editing. The application of this system has been explored beyond genome editing, but there is still plenty of room for improvement for enhancing the specificity and expanding the application of this technology (Ma et al., 2014).

The use of CRISPR-Cas9 technology to engineer THP-1 cells through targeted gene knockout (KO) provides a powerful approach to better characterize immune-related mechanisms, including virus-host interactions. This article describes a protocol for efficient CRISPR-Cas9-based engineering using electroporation to deliver pre-assembled Cas9 sgRNA ribonucleoproteins into the cell nucleus. Up to 95% in protein expression reductions were achieved, and the high editing efficiency of this technique makes it convenient to isolate single-cell clones (Pinaud and Zamborlini, 2025).

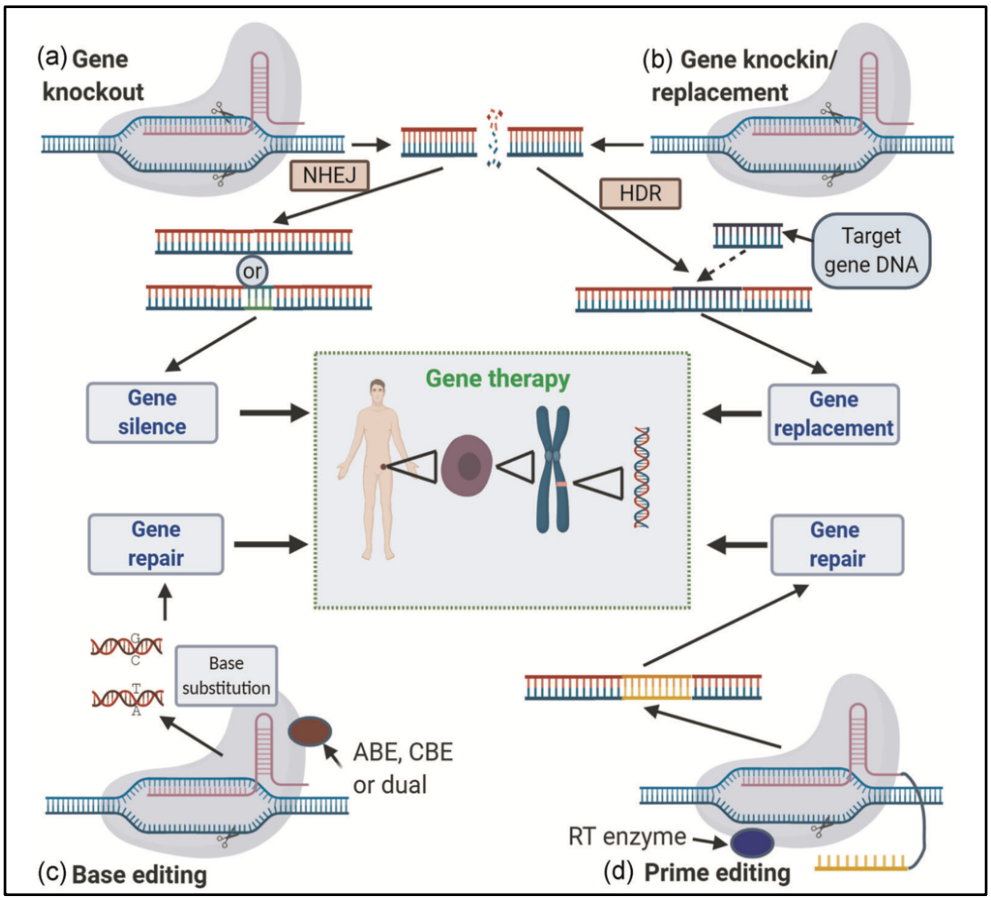

Fig. 2: *Major strategies for CRISPR/Cas9 gene therapy. (a) gene knockout, (b) gene knockin/replacement, (c) base editing, and (d) prime editing* (Zhang, 2021).

Materials and methods

Materials:

GAPDH (Assay ID: Hs02786624_g1, Applied Biosystems, Thermo Fisher Scientific)

DGKA (Assay ID: Hs00176278_m1, Applied Biosystems, Thermo Fisher Scientific)

DGKD (Assay ID: Hs01114141_m1, Applied Biosystems, Thermo Fisher Scientific)

DGKE (Assay ID: Hs00177537_m1, Applied Biosystems, Thermo Fisher Scientific)

DGKG (Assay ID: Hs00176315_m1, Applied Biosystems, Thermo Fisher Scientific)

DGKH (Assay ID: Hs00410739_m1, Applied Biosystems, Thermo Fisher Scientific)

DGKI (Assay ID: Hs01546427_m1, Applied Biosystems, Thermo Fisher Scientific)

DGKQ (Assay ID: Hs01092328_m1, Applied Biosystems, Thermo Fisher Scientific)

DGKZ (Assay ID: Hs05025727_m1, Applied Biosystems, Thermo Fisher Scientific)

DGKK (Assay ID: Hs01385647_m1, Applied Biosystems, Thermo Fisher Scientific)

ACP5 (Assay ID: Hs00356261_m1, Applied Biosystems, Thermo Fisher Scientific)

CAS9 TrueCut™ Cas9 Protein v2 from Thermo, Catalog number: A36499

sgRNA DGKα: 5′-CTCTCAAGCTGAGTGGGTCC-3′

sgRNA DGKζ: 5′-ACGAGCACTCACCAGCATCC-3′

DGKα Rabbit PolyAb, 11547-1-AP, Proteintech

Rabbit Anti-DGKζ pAb, AB105195, Abcam

β-actin Monoclonal Antibody, MA1-140, Invitrogen

1. Cell line and culture condition

The THP-1 cell line identity was verified through a Cell Line Authentication Test conducted by Eurofins Genomics (Ebersberg, Germany), the same cells were used in this study, deriving from the Gorla et al., 2025 article. THP-1 cells were cultured in RPMI-1640 medium (ThermoFisher Scientific, Waltham, MA, USA) supplemented with 10% heat-inactivated fetal bovine serum (FBS, Gibco, cat. no. A5670801) and 1% penicillin-streptomycin (Sigma, cat. no. A5955), following the handling protocols provided by ATCC (Manassas, VA, USA).

1.1 THP-1 differentiation

THP-1 control and edited cell lines were seeded at the concentration of 5×10^5 cells/ml, using RPMI 1640 supplemented with 5% heat-inactivated fetal bovine serum (FBS). During the whole course of the experiment, the medium RPMI 1640 supplemented with

10% heat-inactivated fetal bovine serum (FBS) and 1% penicillin-streptomycin was replaced every 48 hours. Undifferentiated THP-1 cells were used as a control and to verify growth rate they were counted every 48 hours through automated cell counter (TC20TM Automated Cell Counter, BIORAD). To induce differentiation toward macrophage and to promote adhesion, cells were stimulated with PMA at the concentration of 100 ng/ml for 24 hours promoting cell adhesion. THP-1 cells showed highly responsive to DAG-dependent signaling, since their differentiation into macrophages can be easily induced by PMA exposure, a synthetic DAG analog that directly activates protein kinase C (PKC) and mimics endogenous DAG signaling. DAG is unstable and has a short half-life once administered, while its analog PMA exhibits low enzymatic degradation, conferring a strong and long-lasting signal. To further induce differentiation toward osteoclast, cells treated with PMA as indicated were supplemented with M-CSF and RANKL (50 ng/mL each, renewed every 48 hours for 8–10 days). During osteoclastogenesis, cells progressively increased in size and exhibited multinucleation, consistent with osteoclast maturation. At the end of the differentiation process, to evaluate morphology, cells were stained with NucBlue™ (Live Cell Stain ReadyProbes™ reagent, one drop for 500 µl) for fifteen minutes to stain the nuclei, and multiple pictures of every well were acquired with fluorescence microscope [FloydEvos]. Following, cells diameters, nuclei count per cell and cells density were measured in the photos. Cell diameters were measured with FIJI program for at least one hundred cells. The number of nuclei for every cell was manually counted in the same cells as well as the cell density (cells/mm^2).

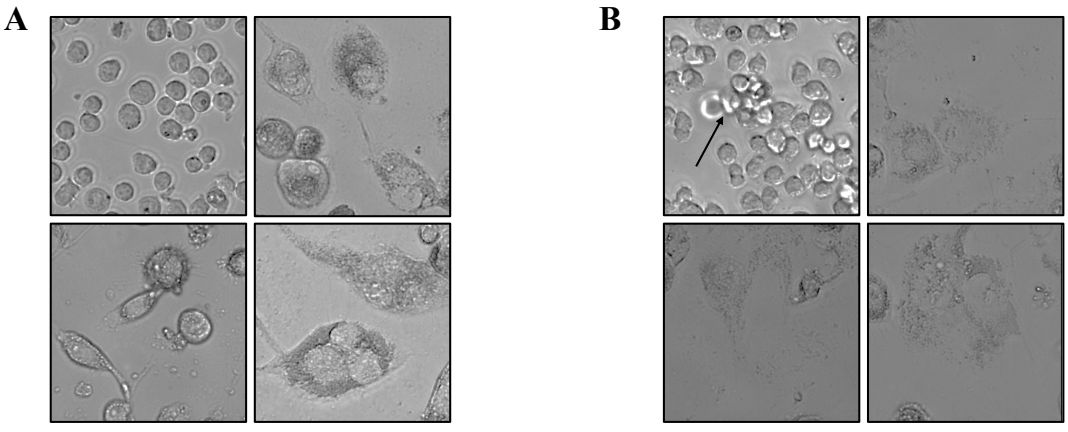

Fig.3: Inclusion and exclusion criteria in cellular spreading and nuclei count measurements

A) Examples of well-defined fields (easily distincted cells).
B) Examples of bad-defined fields specifically excluded from measurement (cells agglomeration, debris, amorphous dying cells).

2. Gene knockdown by CRISPR-Cas9 technology

THP-1 were modified using the CRISPR-Cas9 technology, to obtain a stable culture of knocked-out cells. To edit THP-1 cells we used the P3 Primary Cell 4D-Nucleofector® X Kit S (Lonza). 0.8×10^6 cells for each condition were centrifuged with PBS twice for 10 minutes at 100(G), and a third time without PBS. Then a mix was prepared adding 16.4 µl of P3 Primary Cell Nucleofector® Solution and 3.6 µl of Supplement 1 for each condition in new Eppendorf tubes. Subsequently the mix was added to the guides in the following way: 20 µl of mix + 0.7 µl CAS9 + 0.7 µl of sgRNA or H2O nuclease free.

Later the THP-1 pellet was resuspended with these mixes and added to the Nucleocuvette® Strips and electroporated using the AMAXA (4D-Nucleofecter, Lonza) with a specific program for THP-1 (Amaxa P3 Primary Cell). Electroporated cells were then seeded in a pre-heated 96-well with RPMI-1640 medium supplemented with 10% heat-inactivated fetal bovine serum (FBS) and 1% penicillin-streptomycin and left to grow for some weeks before freezing.

3. Quantitative Real-Time PCR

At the end of the differentiation process cells were lysed in 200 µL of nuclease-free water supplemented with 2% thioglycerol. RNA extraction from lysates was obtained by Kingfisher automated nucleic acid extractor with the MVP_2WASH_200_FLEX protocol and the MagMAXTM Viral/Pathogen Nucleic Acid Isolation Kit (Thermo Fisher). The RNA was then quantified using NanoDrop (Thermo Fisher) and subsequently, equal amounts of RNA were retrotranscribed into cDNA using the High-Capacity cDNA Reverse Transcription Kit (Thermo Fisher) following the manufacturer's instructions. The relative expression of target gene was assessed by quantitative real-time PCR (qRT-PCR) using TaqMan technology. Glyceraldehyde-3-phosphate dehydrogenase (GAPDH) was used as the internal reference gene. qRT-PCR was performed in a 384-well plate using the TaqMan™ Fast Advanced Master Mix kit (Thermo Fisher), 4 µL of mix and 1 µL of cDNA and run on a Bio-Rad CFX384TM (Bio-Rad, Hercules, CA, USA) real-time PCR system. The amplification protocol consisted of an initial denaturation at 95 ◦C for 20 s, followed by 50 cycles of denaturation at 95 ◦C for 3 s and annealing/extension at

60◦C for 30 s. The qRT-PCR reactions were performed in technical triplicates. Data were analyzed with Bio-Rad CFX Maestro 4.1.2433.1219 software.

4. Western Blotting

Cells were lysed in buffer containing HEPES 25 mM, NaCl 150 mM, EDTA 5 mM EGTA 1 mM NP40 1%, and glycerol 10%, supplemented with sodium orthovanadate (1 mM, Thermo Fisher) and protease inhibitor cocktail (0.0089 mg/mL, Sigma Aldrich, St. Louis, MO, USA). Samples were incubated for 15 min at 4◦C, under gentle, constant shaking, and then centrifuged at 12,000× g for 15 min at 4 ◦C. The concentrations of proteins in lysates were quantified by Qubit Protein BR Assay Kit (A50669, Thermo Fisher Scientific, Waltham, MA, USA). Equal amounts of proteins were separated on SDS–PAGE gels and subsequently transferred onto polyvinylidene (PVDF) membranes. Membranes were then blocked with 3% (w/v) BSA for 1 h at room temperature and incubated overnight at 4◦C with the appropriate primary antibodies under gentle agitation. The following day, membranes were washed 3 times in TBS-T buffer and then incubated for 1 h at room temperature with HRP-conjugated rabbit or mouse secondary antibodies (1:5000) under gentle agitation. After three additional washes with TBS-T, the membranes were developed using the Western Chemiluminescence Substrate (PerkinElmer, Shelton, CT, USA) and visualized with the ChemiDoc™ Imaging System (Bio-Rad, Hercules, CA, USA). Band intensities were quantified by densitometry using Bio-Rad Image Lab 6.1 software, normalized to β-actin, and further normalized to the respective controls. Finally, results were analyzed and graphed using GraphPad Prism with two-way ANOVA test.

Results

1. DGK isoforms expression, database exploration

To establish a comprehensive baseline for the DGK isoforms in the THP-1, monocytes and macrophages cells, the Human Protein Atlas was analyzed to provide quantitative RNA-seq data expressed as normalized transcripts per million (nTPM). These are ideal for comparing the different expression of each DGK isoform in the THP-1 cell line, against primary monocytes and macrophages. Complementarily, the FANTOM/CAGE dataset captures promoter-level activity after short-term PMA stimulation, a standard trigger for THP-1 differentiation toward a macrophage-like phenotype.

The graph **A** compares the expression of the different DGK isoforms between the THP-1 cell line, the human monocytes and human macrophages. The most expressed isoform is DGKZ, followed by DGKD and DGKA, while DGKI and DGKK results are not expressed. In the monocytes group, we can see that the most upregulated isoform from the THP-1 group is DGKD, followed by DGKE, DGKG and DGKA; instead the most downregulated is DGKZ, followed by DGKQ and DGKH. Similarly we can compare the macrophages group with the THP-1 group, the most upregulated isoform remains DGKD, followed by DGKA, DGKH and DGKE, the dowregulated ones are primarly DGKZ and then DGKG and DGKQ.

The graph **B** shows the DGK isoforms in THP-1 cells from the FANTOM project, showing similar results from the previous panel, although DGKD results not expressed and DGKG is well expressed. In THP-1 cells treated for 24h with PMA the expression values are similar apart for an increase in DGKI and a decrease in DGKG. For panel **A** and **B** DGKB data are excluded from the analysis, and its values are undetectable.

Those observations indicate that the THP-1 model resembles monocytes and macrophages in terms of DGK isoforms expression, which is also modulable, and the high presence of the DGK isoforms in these cell lines.

A

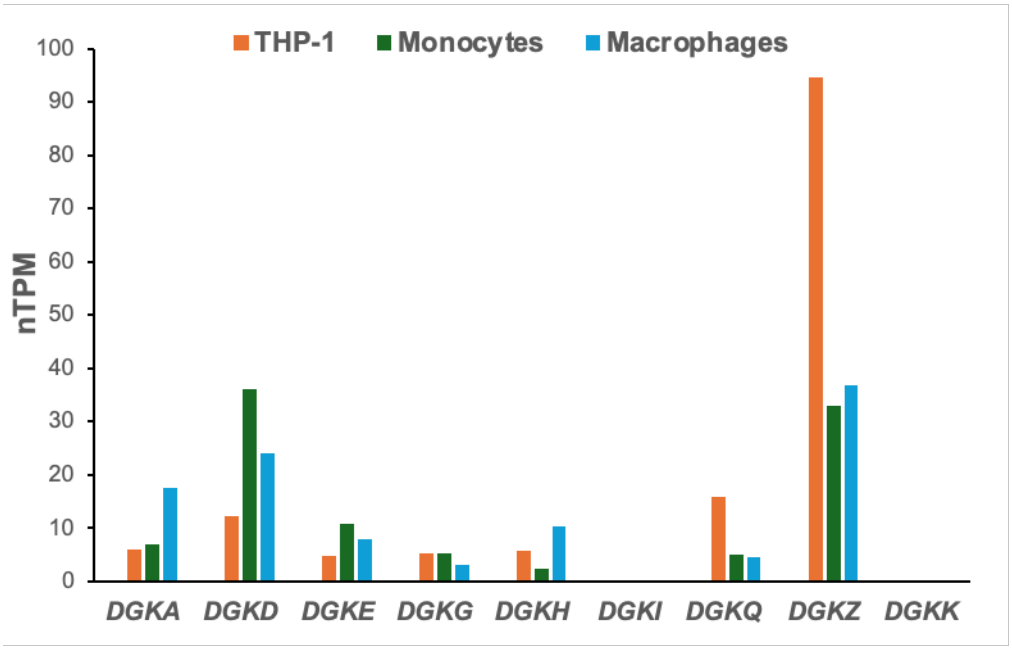

B

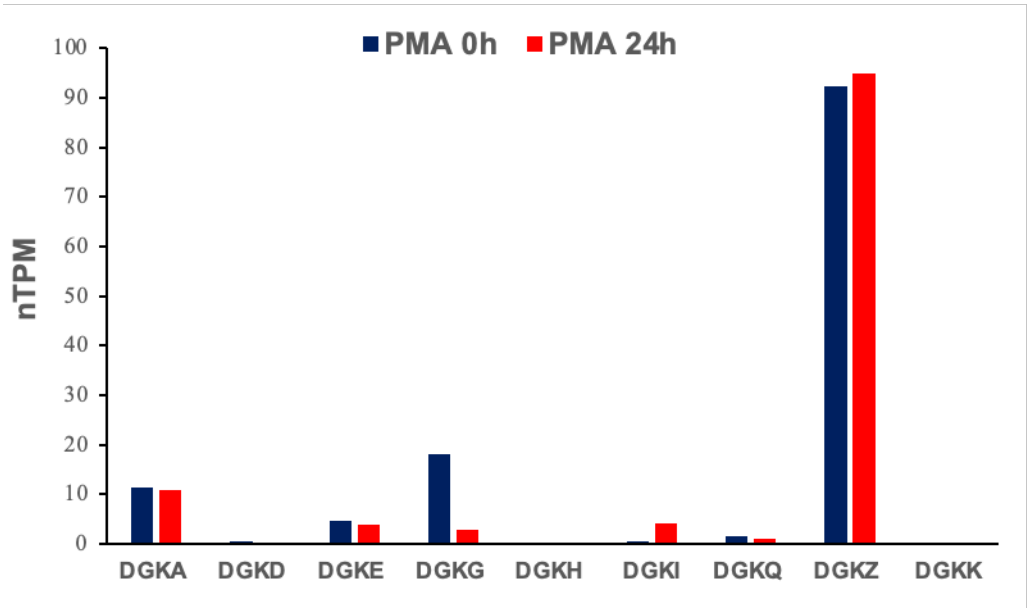

Fig. 4: ***DGK isoforms expression, database exploration***

A. DGKs expression in Human Protein Atlas database as nTPM (Normalized Transcripts Per Million).

B. DGKs expression of THP-1 treated with PMA. Data are obtained from the FANTOM/CAGE dataset and expressed as nTPM (Normalized Transcripts Per Million).

2. DGK isoforms expression during osteoclastogenesis

Subsequently, to further study DGK isoforms expression during osteoclastogenesis, we used the THP-1 cells. They were seeded at the concentration of 0.5×10^6/ml, stimulated with PMA (100 ng/ml) for 24h to induce macrophage differentiation and subsequently treated with M-CSF (50ng/ml) and RANKL (50ng/ml) every 48h for 8-10 days to promote osteoclast differentiation. QRT-PCR was then used to measure the expression of each DGK isoform across the three differentiation stages: THP-1, macrophages and osteoclasts, allowing the identification of the expression patterns during differentiation.

In panel **A** relative expression of DGK isoforms are shown. DGKA expression remained essentially stable throughout differentiation, while DGKD showed a slight reduction in macrophages and osteoclasts and did not reach statistical significance. DGKE and DGKG showed a significant decrease during differentiation and in contrast DGKH did not show a significant variation. DGKI, DGKQ and DGKK showed no statistically significant results, although DGKI and DGKK have an apparent increase. DGKZ, similarly to DGKA, remained relatively constant across all stages, without significant transcriptional modulation. DGKB was barely detectable and its values are not shown.

These observations are in line with the data reported in the databases and guided the selection of DGKα and DGKζ for functional knockout studies. Their expression was maintained throughout differentiation, supporting the hypothesis that their contribution to osteoclastogenesis may depend more on functional activity than on major transcriptional regulation, and therefore most likely to exert a biologically relevant role.

A

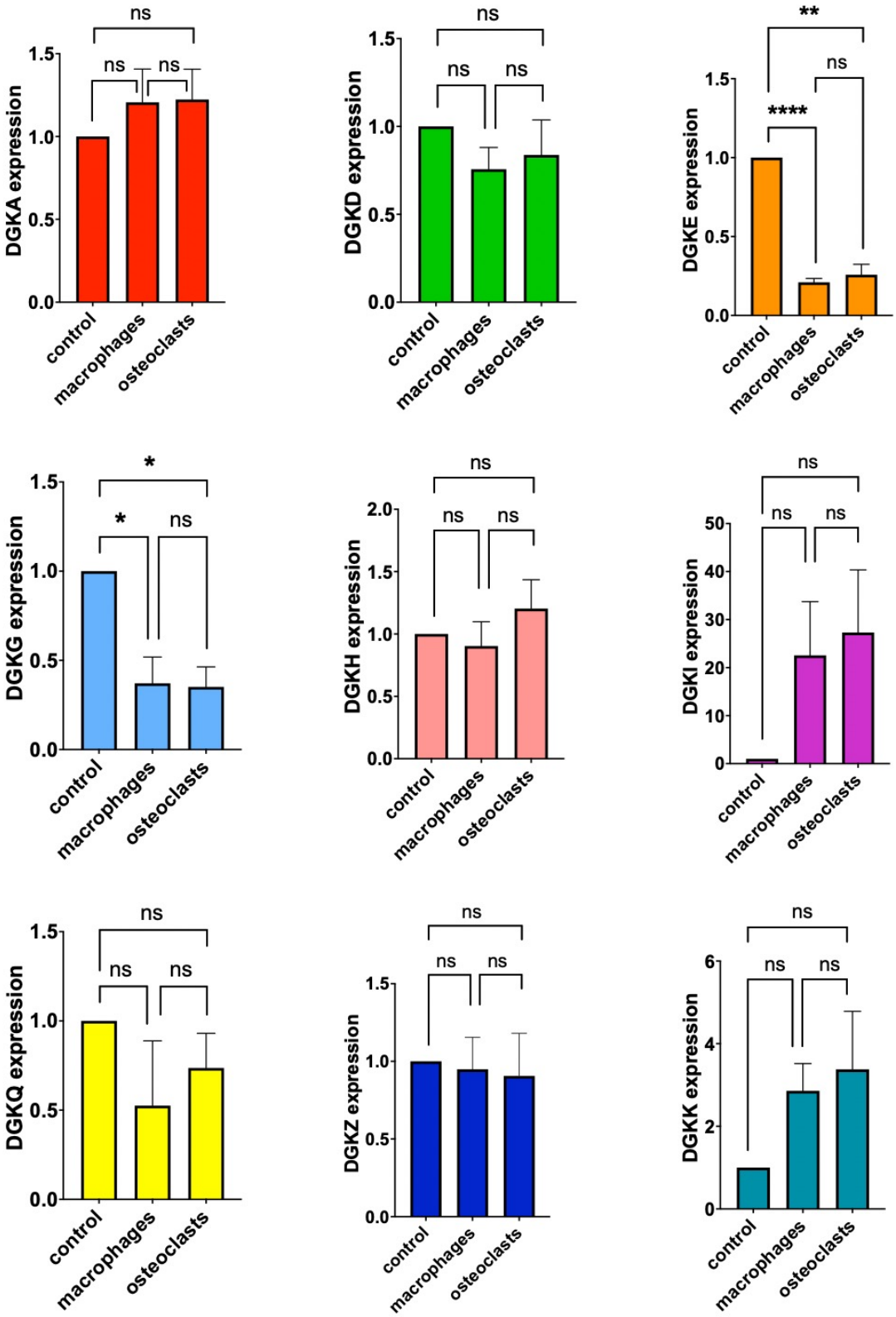

Fig. 5: ***DGK isoforms expression during osteoclastogenesis***

A) DGK isoforms expression, assessed through qRT-PCR, at the end point of the differentiation process at control, macrophages and osteoclasts stages. Data are normalized on "control" and expressed as the mean ± SEM of 3 independent experiments.

3. DGKα and DGKζ knockout on THP-1 cells

THP-1 cells were then knocked out for DGKα and DGKζ by CRISPR/CAS9 technology and differentiated following the previously outlined protocol. Western blotting was then performed to evaluate the knockout effectiveness. In panel **A** data derive from three independent experiments, showing a trend in which both isoforms protein levels increased during differentiation, and a significant reduction in DGKα and DGKζ protein levels.

In DGKα knockout THP-1 protein levels was reduced by ≈ 86% in undifferentiated cells, ≈ 89% in macrophages, and ≈ 85% in osteoclasts, with an overall mean reduction of 87%. Similarly, DGKζ knockout THP-1 achieved reductions of ≈ 90%, ≈ 88%, and ≈ 93% in the same respective conditions, with an overall mean reduction of 91%. In panel **A** there are also representative blots, consistent with the quantitative analysis, showing weaker DGKα and DGKζ bands in knockout samples, while β-actin levels remained comparable among conditions.

Those data demonstrate both the transcriptional modulation of the DGK family in THP-1 differentiation toward osteoclast stage and the successful generation of DGKα and DGKζ deficient THP-1 models for functional studies.

A

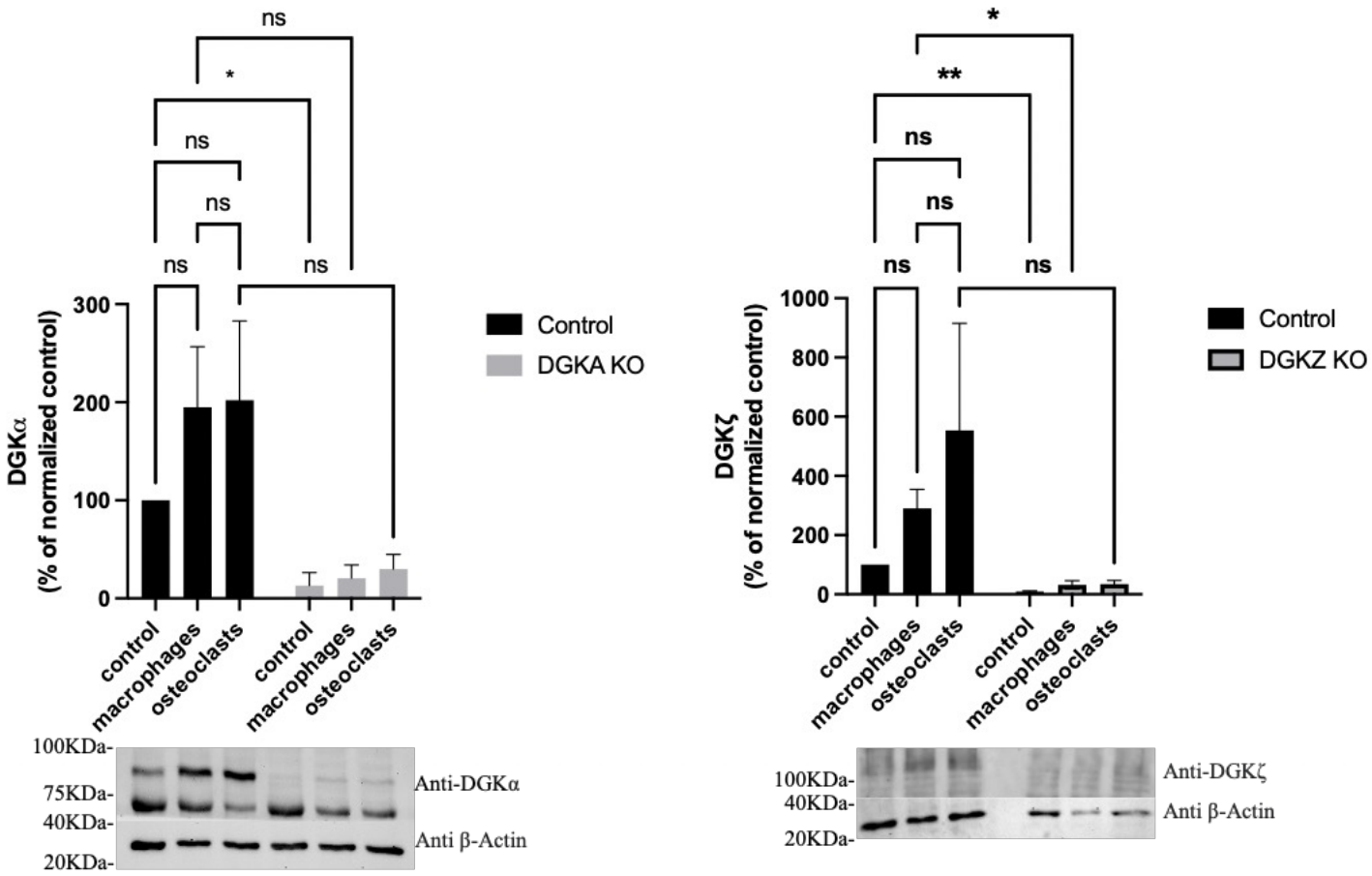

Fig. 6: ***DGKα and DGKζ knockout on THP-1 cells***

A) Western blot analysis between wild-type THP-1 cells and DGKα and DGKζ knockout THP-1 cells, along the differentiation process. Data are obtained from three independent experiments, with mean ± SEM.

4. Role of DGKα and DGKζ in THP-1 growth and density

The next goal was to assess how the loss of DGKα or DGKζ influences the growth capacity of THP-1 undifferentiated cells and their cellular density during the differentiation protocol.

In panel **A** of the **Fig. 7,** cells were counted every 48 hours until the end of the differentiation process to obtain the growth curve among the three conditions. The graph shows that the total live cell counts are comparable, and the knockout of the two DGKs isoform does not impair in a significant manner the THP-1 growth, despite the fact that the knockout cells growth ratio appears lower.

The panel **B** shows the cell density expressed in nuclei/mm^2 evaluated at the end of the differentiation process, presenting a clear reduction of cell density shifting from undifferentiated cells to the macrophages and osteoclast stage. The cell density trend is similar among the three conditions, and the significant increase from macrophages control to osteoclasts control suggest that DGKα and DGKζ may play a role in the fusion and the multinucleation course of action. For both panels data derives from a mean of three independent experiments.

Overall, panel **A** and **B** suggest that DGKα and DGKζ are required for efficient THP-1 cell expansion during osteoclastogenic differentiation, while they do not substantially affect the final cell density. Therefore **Fig. 7** links DGKα and DGKζ expression to both basal proliferation and the ability to loose the high cellular density following the formation of mature osteoclasts.

A

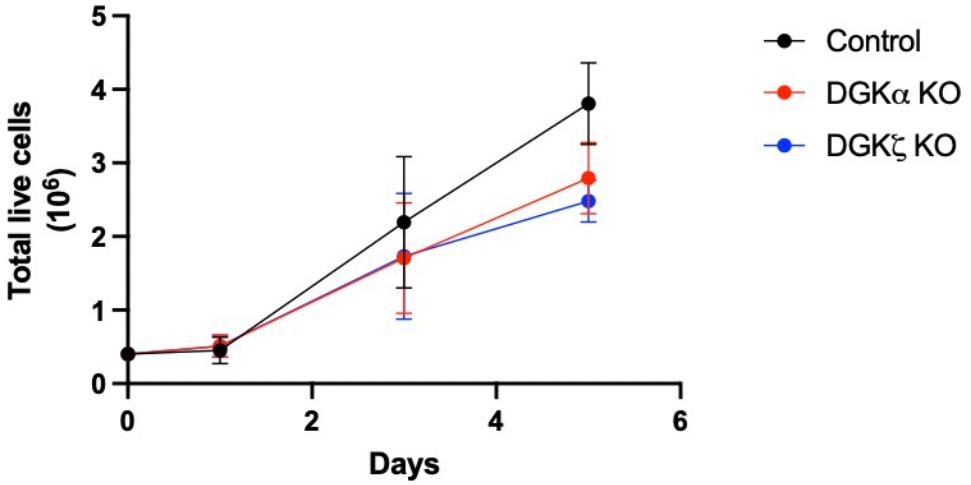

B

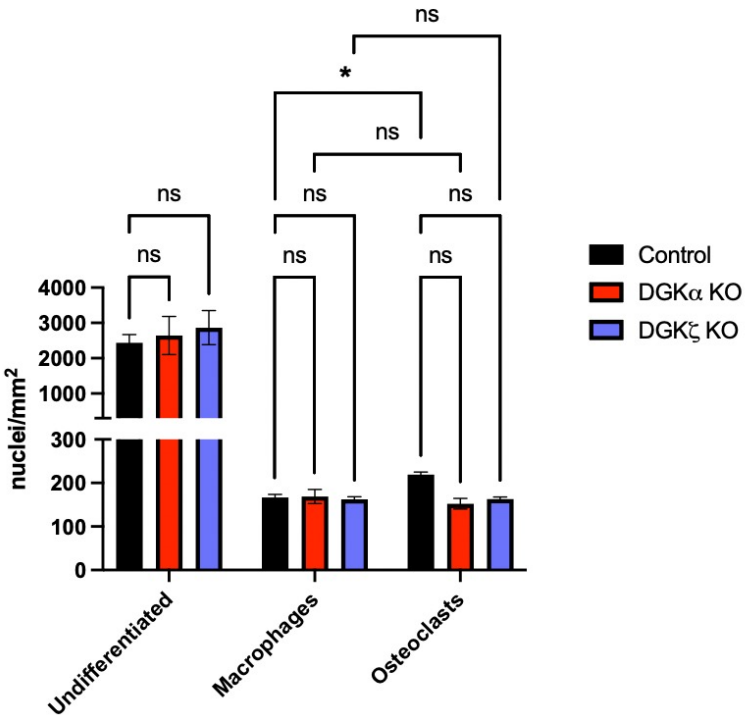

Fig. 7: ***Role of DGKα and DGKζ in THP-1 growth and density***

After the knockout of DGKα and DGKζ on THP-1, cells were seeded at the concentration of 0.5 x 10^6/ml. They were then stimulated with PMA (100 ng/ml) for 24h to induce macrophage differentiation and subsequently, MCSF (50ng/ml) and RANKL (50ng/ml) were added every 48h for 8-10 days to promote osteoclastogenesis.

A) Total live cell counts of undifferentiated THP-1 cells. Data are obtained from the mean of three independent experiments ± SEM.

B) Cell density expressed in nuclei/mm^2 evaluated at the end of the differentiation process. Data are obtained from the mean of three independent experiments ± SEM.

5. Role of DGKα and DGKζ in THP-1 osteoclastogenesis

This multi-panel figure provides a comprehensive phenotypic characterization of DGKα and DGKζ deficient THP-1 cells after the full osteoclast differentiation protocol. Collectively, **Fig. 8** integrates morphological, molecular, and quantitative metrics to demonstrate that DGKα and DGKζ are essential regulators of the cell size, nuclear content, and differentiation marker regulator in the osteoclastogenesis of THP-1 cells.

The representative images in panel **A** are taken at the end of the differentiation process illustrating the morphological characteristics of the three cell lines. In the control group THP-1 cells displayed a normal phenotype and successfully formed large, multinucleated syncytia while differentiating towards macrophages and then osteoclast stage. In DGKα and DGKζ KO cells we observed an increased presence of cellular debris compared to the controls, a statistically significant reduction of cells size and in general the differentiation process failed to achieve the morphological complexity of the THP-1 control group.

In the panel **B** is evaluated the differentiation status of the cells by the expression of Tartrate-Resistant Acid Phosphatase (TRAP), marker for functional osteoclasts, via qRT-PCR. In the control group the TRAP gene expression rises in the macrophage and osteoclast stage showing successfull differentiation. In DGKα and DGKζ knockout cells we can see a similar trend, but the gene expression is significantly higher compared to the control group, suggesting a role of the DGKs in the differentiation process. In addition, the expression of CathepsinK, another key osteoclastic marker involved in bone matrix degradation, was also evaluated; however, no significant or consistent changes were observed during the induction process, suggesting that under the applied experimental conditions its expression was not markedly modulated.

The violin plot in the panel **C** represents the morphological analysis of the diameter lenghts of at least 100 cells per condition. In the control group, undifferentiated THP-1 cells have a median diameter lenght of approximately 18 μm, which increased to approximately 70 μm in macrophages and 80 μm in osteoclasts. DGKα KO cells are approximately 18 μm for undifferentiated cells, 70 μm for macrophages and 75 μm for osteoclasts. In contrast, DGKζ KO cells showed a slight reduction at every stage, with undifferentiated cells at approximately 16 μm, macrophages at 55 μm, and osteoclasts at

65 μm. In the control group we can observe a clear and significant increase in diameter size, both for macrophages and osteoclast compared to undifferentiated THP-1. For both the DGKα and DGKζ knockout groups, the macrophages are significantly bigger than the undifferentiated THP-1, but the osteoclast are comparable to the macrophages, key difference from the control group. In general, there's also a significant reduction of cell size between the three conditions: macrophages and osteoclast diameters from the DGKα and DGKζ knockout groups are smaller compared to the control ones.

Similar trends can be observed in the violin plot of the panel **D**, that shows the number of nuclei per cell, exploring the multinucleation and the fusion ability of the three groups. In the control group there's a clear increase of the number of nuclei, both for macrophages and for osteoclast, and the same happens in the DGKα and DGKζ knockout groups. Instead we can see that the macrophages of the DGKα and DGKζ knockout groups are comparable to the control one, but the osteoclast stage seems to be significantly lower in the knockout groups compared to the control. For both **C** and **D** panels data derives from a mean of three independent experiments.

Together, these four graphs: representative images, cell diameter and nuclei count, together with TRAP expression allows a comprehensive evaluation of how DGKα and DGKζ control the formation of competent osteoclasts in the THP-1 cell line.

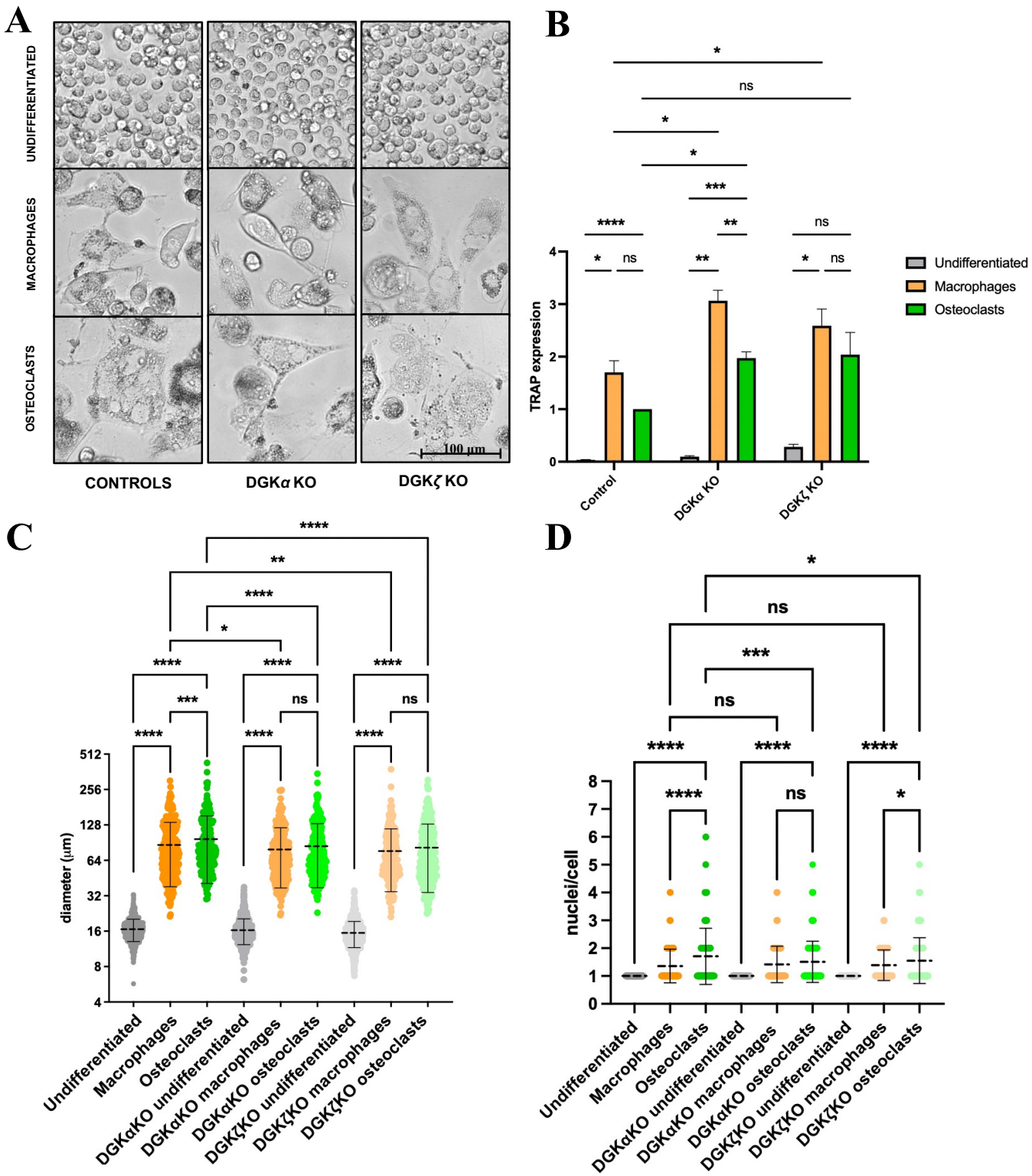

Fig. 8 : ***Role of DGKα and DGKζ in THP-1 osteoclastogenesis***

After the knockout of DGKα and DGKζ on THP-1, cells were seeded at the concentration of 0.5 x 10^6/ml. They were then stimulated with PMA (100 ng/ml) for 24h to induce macrophage differentiation and subsequently, MCSF (50ng/ml) and RANKL (50ng/ml) were added every 48h for 8-10 days to promote osteoclastogenesis.

A) Representative images taken at the end of the differentiation process.

B) Levels of TRAP expression, assessed through qRT-PCR, at the end point of the differentiation process at undifferentiated, macrophages and osteoclasts stages. Data are normalized on "osteoclast control" and expressed as the mean ± SEM of 3 independent experiments.

C) Violin plot showing the maximum diameter length of >100 cells per condition. Data are from three independent experiments, with mean ± SEM.

D) Each sample was stained with NucBlue to allow nuclei identification. Data are from three independent experiments, with mean ± SEM.

Discussion

The present study wants to clarify DGKα and DGKζ role to the osteoclastogenic differentiation of THP-1 cells, starting from the hypothesis that the loss of these two isoforms could alter the transition from monocytic cells to macrophages and finally to osteoclast-like cells under PMA, M-CSF and RANKL stimulation. This hypothesis was biologically plausible since the introductory framework of the thesis had highlighted a relevant role of DGKs in macrophage regulation and suggested a possible involvement of DGKs dependent signaling in osteoclastogenesis.

The **Fig. 4** derives from databases exploration of Human Protein Atlas and FANTOM/CAGE data. The first one explores the values of nine different DGK isoforms in THP-1, monocytes, macrophages and expressed as nTPM; the second one focuses only on THP-1 cells, treated with PMA for 24h or non treated. Considering both data, DGKZ is the highest expressed isoform across, followed by DGKA, DGKG, DGKD, DGKE and DGKQ, while the other isoforms are poorly expressed. Subsequently, qRT-PCR was performed on THP-1 cells along their differentiation protocol, with PMA used to induce macrophage commitment and M-CSF plus RANKL to promote osteoclastogenesis, over a period of 8 to 10 days. In **Fig. 5** the expression values of DGKA, DGKD, DGKE, DGKG, DGKH, DGKI, DGKQ, DGKZ and DGKK are showed. We saw significant reduction in DGKE and DGKG expression values during osteoclastogenesis, whereas other isoform revealed stable values, or non-significant upwards or downwards trends. To provide a more comprehensive overview, a comparative table summarizes the behavior of all nine DGK isoforms across **Fig. 4** and **Fig. 5**. The values from qRT-PCR are concordant with databases in DGKA, DGKG, DGKH, DGKQ and DGKZ. Instead, DGKI is partially similar, and the other isoforms values are substantially different. The partial overlap observed likely reflects the intrinsic differences between publicly available transcriptomic datasets and targeted experimental measurements. In particular, variations in sample source, methodological platform, normalization approach, and differentiation stages are all likely to contribute to the discordant patterns observed for several isoforms. The comparative table can be interpreted as a framework for discussion of general expression trends and isoform-specific divergences, rather than an evidence of direct quantitative equivalence among the datasets.

Isoform	Fig. 4A: Human Protein Atlas (nTPM)	Fig. 4B: FANTOM/CAGE (nTPM)	Fig. 5: qRT-PCR	Coherence
DGKA	Moderate in THP-1 (~7) and monocytes (~7); increased in macrophages (~18)	Stable before and after PMA treatment (~10-11)	Slight upward trend in macrophages and osteoclasts	Concordant
DGKD	Peak in monocytes (~36); macrophages (~24); THP-1 (~12)	Very low	Slight decrease in macrophages and osteoclasts	Discordant
DGKE	Low across all cell types (5-10)	Low and stable in THP-1 (~4-5)	Significant decrease in macrophages and osteoclasts vs. control	Discordant
DGKG	Low expression (3-6); slightly reduced in macrophages	Strong decrease after PMA treatment in THP-1 (from ~18 to ~3)	Significant decrease in macrophages and osteoclasts vs. control	Concordant
DGKH	Low and variable (2-10)	Very low	Near-control levels in macrophages and osteoclasts	Concordant
DGKI	Very low	Slight increase after PMA treatment (from ~1 to ~4)	Substantial increase in macrophages and osteoclasts	Partial
DGKQ	Moderate in THP-1 (~16); reduced in monocytes and macrophages (~5)	Very low	Decrease in macrophages; partial recovery in osteoclasts	Concordant
DGKZ	Highest isoform in THP-1 (~95); reduced in monocytes (~33) and macrophages (~37)	High and stable (~92-95)	Stable across all conditions	Concordant
DGKK	Very low	Very low	Upward trend in macrophages and osteoclasts	Discordant

Fig. 9: *Comparative table between public databases and qRT-PCR*

After this comprehensive review, we decided to choose DGKα and DGKζ for the next studies, further supported by the introduction part where there is evidence of their relevance in macrophage and osteoclast regulation, together with the values deriving from the databases. In parallel, the expression analysis performed with qRT-PCR demonstrated that both DGKα and DGKζ expression remain relatively stable across the undifferentiated, macrophage and osteoclast stages. This suggests that their contribution to osteoclastogenesis is not necessarily linked to a large transcriptional oscillation, but may instead depend on a constitutive functional role in intracellular signaling events coming with differentiation.

THP-1 cells were edited through CRISPR-Cas9 technology, and then subjected to the standardized differentiation protocol. The efficacy of the knockout was confirmed by western blotting in **Fig. 6**, showing a strong reduction in DGKα and DGKζ protein levels (respectively 87% and 91%). Moreover, in THP-1 cells the protein levels tend to increase when shifting to macrophage and osteoclast stages, whereas in the KO groups this trend is not maintained. Therefore, the phenotypic changes observed in the edited cells can reasonably be interpreted as a consequence of DGKα or DGKζ depletion, although some residual cells expressing the targets are still present.

Since total live cell counts, as well as cell density (nuclei/mm^2), did not differ significantly among control and knockout conditions in **Fig. 7**, DGKα and DGKζ are not strictly required for cell survival or for the maintenance of a minimal proliferative capacity in THP-1 cells. Indeed, our work group have previously demonstraded that DGKα and DGKζ silencing minimally enhanced apoptosis in THP-1 cells compared to control cells, whereas necrosis remained negligible under all conditions (Gorla et al., 2025). Thus, in THP-1 cells, decreasing DGKα and DGKζ protein levels do not significantly impair cell viability, suggesting a non-essential or functionally redundant role of these isoforms in this cellular context. However, their loss becomes much more relevant once cells are challenged to complete the osteoclastogenic program. Control THP-1 cells underwent the expected phenotypic transition and generated large multinucleated syncytia, whereas DGKα KO and DGKζ KO cells showed increased cellular debris, reduced spreading and a general inability to reach the same degree of morphological complexity. This indicates that DGKα and DGKζ are less important for basal growth, but relevant in the structural remodeling required to generate osteoclast-like cells.

The analysis in **Fig. 8** further strengthens this conclusion. In control cells, the increase in cell diameter observed during differentiation was marked, with osteoclasts becoming substantially larger than the undifferentiated THP-1 population. By contrast, in both DGKα KO and DGKζ KO cells, macrophages were larger than undifferentiated cells, but the subsequent transition from macrophage to osteoclast was much less pronounced, and the final osteoclast population remained significantly smaller than the control counterpart. This pattern suggests that the absence of DGKα and DGKζ does not completely abolish the initial response to differentiation stimuli, but specifically compromises the later stages, associated with full cytoplasmic expansion and cell fusion. A similar interpretation emerges from the analysis of multinucleation. In all three groups, the number of nuclei per cell increased during differentiation, showing some degree of progression along the osteoclastogenic pathway. Nevertheless, the osteoclast stage of DGKα KO and DGKζ KO cells displayed significantly fewer nuclei per cell compared to control osteoclasts. Since multinucleation is a defining feature of mature osteoclasts, this result strongly supports the idea that both DGKα and DGKζ are functionally involved in fusion-related events that control the formation of fully developed osteoclast-like syncytia.

TRAP, a classical osteoclast marker and a downstream readout of osteoclastogenic differentiation, increased in control cells during the induction process as expected. However, TRAP expression was significantly higher in DGKα KO and DGKζ KO cells than in controls, despite the fact that these cells failed to achieve normal size and multinucleation. This finding suggests that DGKα and DGKζ depletion does not simply suppress osteoclast-associated transcription, but may instead generate a partially uncoupled phenotype in which some molecular components of the differentiation program are activated while the morphological and functional completion of the osteoclast state remains impaired. Moreover, the absence of clear modulation in CathepsinK expression instead points to an altered or incomplete maturation program in this cellular model. These data are coherent with the idea that DGKα and DGKζ regulate signaling pathways rather than acting as simple on or off switches for osteoclastogenesis. DGKs control the balance between DAG and PA, and this balance is likely to be particularly important during stages of differentiation that require extensive membrane remodeling, cytoskeletal reorganization, cell spreading and precursor fusion. From this point of view, the increased TRAP expression observed in knockout cells may reflect an attempt to engage the osteoclastogenic program, while the reduced cell size and lower multinucleation reveals an inability to execute the full structural program needed for mature osteoclast formation.

In particular, in the introduction there is evidence that in DGKα knockout mice, DGKα acted as a regulator of macrophage activation, increasing their responsiveness. In the wound healing process, the wounds were smaller and showed an increase in the number of local macrophages. This can be justified as an increased cell cycling, migration and influx of DGKα knockout macrophages at wound sites (Manigat et al., 2021). DAG-related pathways are also involved in bone remodeling. For intance, M-CSF, induces the generation of DAG, necessary for c-Fos expression, a transcription factor involved in osteoclast differentiation. Moreover, DGKζ knockout mice are osteoporotic due to a marked increase in osteoclast number, while in vitro DGKζ knockout bone marrow macrophages form more numerous, larger and highly resorptive osteoclasts. DGKζ deficiency increases responsiveness to the proliferative and pro-survival cytokine M-CSF (Zamani et al., 2015). In contrast, in the THP-1 model, the loss of DGKζ, as well as the loss of DGKα, was associated with impaired morphological maturation. We expected that

blocking DGK activity would increase the DAG inside the cells, enhancing the osteoclastogenic differentiation of THP-1 cells. Moreover THP-1 are also highly responsive to DAG-dependent signaling, since their differentiation into macrophages can be easily induced by PMA exposure, a synthetic DAG analog that directly activates PKC and mimics endogenous DAG signaling.

This apparent discrepancy with the literature can be explained because these studies were performed in biological settings that differ substantially from the present model, including species, precursor origin, differentiation system, and experimental readout. Bone marrow macrophages from knockout mice are primary cells that undergo osteoclastogenesis in a physiological myeloid context, whereas THP-1 cells are an immortalized human monocytic leukemia cell line that reproduces only selected aspects of macrophage and osteoclast-like differentiation. In our model, osteoclast-like differentiation occurs in a simplified monoculture setting, without stromal cells, osteoblasts, endothelial cells, lymphocytes, or other components of the bone and inflammatory microenvironment. This means that the process limiting osteoclast accumulation in vivo may not be identical to the process limiting multinucleation or spreading in vitro. A reduced ability of individual cells to spread or fuse in monoculture could still coexist, in a more complex in vivo environment, with signals that increase precursor recruitment, survival, or osteoclast-supportive niche interactions. For this reason, the increased osteoclast number seen in DGKζ deficient mice by Zamani et al., (2015), does not necessarily imply that every in vitro system should display the same direction of change in cell size or nuclear content. The differences may also indicate that DGKs dependent signaling has context-specific effects. In primary murine osteoclast precursors, the DAG accumulation following DGKζ loss enhances M-CSF-dependent proliferative and survival pathways, thereby increasing the pool of osteoclast precursors and promoting osteoclast formation. In THP-1 cells, the same disruption of the DAG/PA balance may interfere with later events that depend on coordinated membrane dynamics and cytoskeletal remodeling, such as cell spreading and fusion. However, the key issue here is not simply that THP-1 cells differ from primary precursors, but that the two models may emphasize different stages of the differentiation process. In our setting, DGKζ may mainly affect late fusion-dependent and morphological maturation events, whereas constitutive DGKζ deficiency in primary murine precursors described by Zamani et al., (2015) may reshape the osteoclastogenic program from earlier

stages. This could produce a phenotype in which transcriptional markers such as TRAP are activated, but morphological maturation remains defective. In this sense, the present results suggest that DGKα and DGKζ are required in THP-1 cells for the acquisition of mature osteoclast-like morphology, even though their loss may have different consequences in primary murine systems.

Another relevant aspect of the study is that both DGKα and DGKζ knockout produced a broadly similar phenotype. This convergence suggests that the two isoforms may each contribute to the proper execution of osteoclast maturation, either through partially overlapping functions or through distinct signaling pathways that ultimately affect the same cellular outputs. It would be interesting in this way to study separately DGKα and DGKζ deficient mice, in order to clarify in vivo the specific role of each isoform in osteoclast activity and skeletal homeostasis.

Within the same research group, the roles of DGKα and DGKζ were further investigated through DGKα and DGKζ inhibition with the use of ritanserin and BAY 2965501 in THP-1 cells. The results are closely related to the ones coming from the knockout of these isoforms, reinforcing even more the accuracy of these findings. In both cases, DGKα or DGKζ impairment does not completely abolish the response of THP-1 cells to osteoclastogenic stimulation, but it reduces the acquisition of mature osteoclast-like morphology. In both models, treated cells showed an increase in cellular debris and a general reduced cellular complexity during THP-1 osteoclastogenesis. Instead, TRAP expression behaves differently between the two settings. In this model, TRAP expression was increased in DGKα KO and DGKζ KO cells, whereas in the inhibitor-treated cells, TRAP expression appears not significantly enhanced. A direct comparison of both panels regarding cell spreading and multinucleation further supports this interpretation. In DGKα KO and DGKζ KO cells, as well as for the pharmacological inhibition, cells showed a reduced increase in diameter compared with control osteoclasts, indicating impaired cytoplasmic expansion during the late phase of differentiation. Similarly, inhibitor-treated cells also showed a comparable reduction in nuclei number, reinforcing the idea that both genetic and pharmacological impairments of DGKα and DGKζ mainly affect the late fusion-dependent phase of THP-1 osteoclast-like maturation.

Overall, the results of this thesis support the conclusion that DGKα and DGKζ are important regulators of osteoclast maturation in THP-1 cell model. Their depletion does not abolish the entire differentiation response, but it compromises the acquisition of the main structural features defining mature osteoclast-like cells, particularly cell enlargement and multinucleation. The most convincing interpretation is therefore that DGKα and DGKζ are required for the efficient completion of the osteoclastogenic program rather than for its initial triggering alone. In this sense, the study adds new evidence that DGKs dependent signaling is relevant to the osteoclast-like differentiation and identifies DGKα and DGKζ as functionally key regulators of osteoclast maturation in THP-1 cells.

Finally, the design of this work, which included DGKs expression, knockout validation, gene expression analysis, growth evaluation, cell density analysis, morphometry and nuclei counting, provides a solid basis for future investigations aimed at linking these phenotypic changes to specific signaling mechanisms. Future studies will be important to determine whether the morphological defect observed is accompanied by parallel defects in bone resorption capacity, cytoskeletal organization or responsiveness to osteoclastogenic cytokines, and to clarify whether DGKα and DGKζ act through shared or partially distinct downstream pathways. Moreover, further studies in primary osteoclasts and in vivo models will be important to validate the present findings and better define the role of DGKα and DGKζ in osteoclastogenesis.

Bibliography

- Diepenhorst, N.A., Nowell, C.J., Rueda, P., Henriksen, K., Pierce, T., Cook, A.E., Pastoureau, P., Sabatini, M., Charman, W.N., Christopoulos, A., et al. (2017). High throughput, quantitative analysis of human osteoclast differentiation and activity. Anal. Biochem.519, 51–56.
- Pereira, M., Petretto, E., Gordon, S., Bassett, J.H.D., Williams, G.R., and Behmoaras, J. (2018). Common signalling pathways in macrophage and osteoclast multinucleation. J. Cell Sci.131, jcs216267.
- Omi, M., and Mishina, Y. (2022). Roles of osteoclasts in alveolar bone remodeling. Genesis60, e23490.
- Søe, K., Delaisse, J.-M., and Borggaard, X.G. (2021). Osteoclast formation at the bone marrow/bone surface interface: Importance of structural elements, matrix, and intercellular communication. Semin. Cell Dev. Biol.112, 8-15.
- Mun, S.H., Park, P.S.U., and Park-Min, K.-H. (2020). The M-CSF receptor in osteoclasts and beyond. Experimental & Molecular Medicine 52, 1239-1254.
- Park, J.H., Lee, N.K., and Lee, S.Y. (2017). Current understanding of RANK signaling in osteoclast differentiation and maturation. Mol. Cells40, 706–713.
- Ono, T., and Nakashima, T. (2018). Recent advances in osteoclast biology. Histochem. Cell Biol.149, 325–341.
- Miyamoto, T. (2011). Regulators of osteoclast differentiation and cell-cell fusion. Keio J. Med.60, 101–105.
- Ethiraj, L.P., Fong, E.L.S., Liu, R., Chan, M., Winkler, C., and Carney, T.J. (2022). Colorimetric and fluorescent TRAP assays for visualising and quantifying fish osteoclast activity. Eur. J. Histochem.66, 3369.
- Drake, M.T., Clarke, B.L., Oursler, M.J., and Khosla, S. (2017). Cathepsin K inhibitors for osteoporosis: Biology, potential clinical utility, and lessons learned. Endocr. Rev.38, 325–350.
- Liu, J., Ma, J., Zhang, Y., Li, J., Yang, Y., Yin, P., Wan, X., Ma, S., and Shang, D. (2025). DGKs in lipid signaling and disease intervention: structural basis, pathological mechanisms, and emerging therapeutic strategies. Cell. Mol. Biol. Lett.30, 129.
- Sim, J.A., Kim, J., and Yang, D. (2020). Beyond Lipid Signaling: Pleiotropic Effects of Diacylglycerol Kinases in Cellular Signaling. Int. J. Mol. Sci.21, 6861.
- Xie, S., Naslavsky, N., and Caplan, S. (2015). Diacylglycerol kinases in membrane trafficking. Cell. Logist.5, e1078431.
- Racca, L., Baldanzi, G., and Massarotti, A. (2025). Modulators of diacylglycerol kinase activity: A review of advances and challenges. Med. Res. Rev.46, 149–175.
- Sakane, F., Hoshino, F., and Murakami, C. (2020). New era of diacylglycerol kinase, phosphatidic acid and phosphatidic acid-binding protein. Adv. Biol. Regul.78, 100744.

- Lee, H.J., and Zheng, J.J. (2010). PDZ domains and their binding partners: structure, specificity, and modification. Cell Commun. Signal.8, 8.
- Gravina, T., Boggio, C.M.T., Gorla, E., Racca, L., Polidoro, S., Centonze, S., Ferrante, D., Lunghi, M., Graziani, A., Corà, D., and Baldanzi, G. (2023). Role of Diacylglycerol Kinases in Acute Myeloid Leukemia. Biomedicines11, 1877.
- Baldanzi, G., and Malerba, M. (2019). DGKα in Neutrophil Biology and Its Implications for Respiratory Diseases. Int. J. Mol. Sci.20, 5673.
- Fazio, A., Obeng, E.O., Rusciano, I., Marvi, M.V., Zoli, M., Mongiorgi, S., Ramazzotti, G., Follo, M.Y., McCubrey, J.A., Cocco, L., et al. (2020). Subcellular Localization Relevance and Cancer-Associated Mechanisms of Diacylglycerol Kinases. Int. J. Mol. Sci.21, 5297.
- Nakano, T., Matsui, H., Tanaka, T., Hozumi, Y., Iseki, K., Kawamae, K., and Goto, K. (2016). Arachidonoyl-Specific Diacylglycerol Kinase ε and the Endoplasmic Reticulum. Front. Cell Dev. Biol.4, 132.
- Zamani, A., Decker, C., Cremasco, V., Hughes, L., Novack, D.V., and Faccio, R. (2015). Diacylglycerol Kinase ζ (DGKζ) Is a Critical Regulator of Bone Homeostasis Via Modulation of c-Fos Levels in Osteoclasts. J. Bone Miner. Res.30, 1852–1863.
- Gorla, E., Cartella, M.C., Borghetti, E., Lovati, G., Racca, L., Gravina, T., Biazzo, G., Bonello, G., Malacarne, V., De Giorgis, V., et al. (2025). Acute Myeloid Leukemia: A Key Role of DGKα and DGKζ in Cell Viability. Cells14, 1721.
- Manigat, L.C., Granade, M.E., Taori, S., Miller, C.A., Vass, L.R., Zhong, X.P., Harris, T.E., and Purow, B.W. (2021). Loss of diacylglycerol kinase α enhances macrophage responsiveness. Front. Immunol.12, 722469.
- Mahajan, S., Mellins, E.D., and Faccio, R. (2020). Diacylglycerol kinase ζ regulates macrophage responses in juvenile arthritis and cytokine storm syndrome mouse models. J. Immunol.204, 137–146.
- Okada, M., Hozumi, Y., Iwazaki, K., Misaki, K., Yanagida, M., Araki, Y., Watanabe, T., Yagisawa, H., Topham, M.K., Kaibuchi, K., et al. (2012). DGKζ is involved in LPS-activated phagocytosis through IQGAP1/Rac1 pathway. Biochem. Biophys. Res. Commun.420, 479–484.
- Yamada, K., Sakane, F., Imai, S., Tsushima, S., Murakami, T., and Kanoh, H. (2003). Regulatory role of diacylglycerol kinase ζ in macrophage differentiation of leukemia cells. Biochem. Biophys. Res. Commun.305, 101–107.
- McNally, A.K., and Anderson, J.M. (2003). Foreign body-type multinucleated giant cell formation is potently induced by α-tocopherol and prevented by the diacylglycerol kinase inhibitor R59022. Am. J. Pathol.163, 1147–1156.
- Kweon, H., Kim, S.G., and Choi, J.Y. (2014). Inhibition of foreign body giant cell formation by 4-hexylresorcinol through suppression of diacylglycerol kinase delta gene expression. Biomaterials35, 8576–8584.

- Yang, Z., Kim, S., Mahajan, S., Zamani, A., and Faccio, R. (2017). Phospholipase C-γ1 controls osteoclast numbers via colony-stimulating factor 1-dependent diacylglycerol/β-catenin/cyclinD1 pathway. J. Biol. Chem.292, 1178–1186.
- Liu, T., Huang, T., Li, J., Li, A., Li, C., Huang, X., Li, D., Wang, S., and Liang, M. (2023). Optimization of differentiation and transcriptomic profile of THP-1 cells into macrophage by PMA. PLoS ONE18, e0286056.
- Li, Z.H., Si, Y., Xu, G., Chen, X.M., Xiong, H., Lai, L., Zheng, Y.Q., and Zhang, Z.G. (2017). High-dose PMA with RANKL and MCSF induces THP-1 cell differentiation into human functional osteoclasts in vitro. Mol. Med. Rep.16, 8380–8384.
- Chanput, W., Mes, J.J., and Wichers, H.J. (2014). THP-1 cell line: An in vitro cell model for immune modulation approach. Int. Immunopharmacol.23, 37–45.
- Forrester, M.A., Wassall, H.J., Hall, L.S., Cao, H., Wilson, H.M., Barker, R.N., and Vickers, M.A. (2018). Similarities and differences in surface receptor expression by THP-1 monocytes and differentiated macrophages polarized using seven different conditioning regimens. Cell Immunol.332, 58–76.
- Mohd Yasin, Z.N., Mohd Idrus, F.N., Hoe, C.H., and Yvonne-Tee, G.B. (2022). Macrophage polarization in THP-1 cell line and primary monocytes: A systematic review. Differentiation128, 67–82.
- Wang, H., and Shen, Y. (2019). MicroRNA-20a negatively regulates the growth and osteoclastogenesis of THP-1 cells by downregulating PPARgamma. Mol. Med. Rep.20, 4271–4276.
- Zhang, B. (2021). CRISPR/Cas gene therapy. J. Cell. Physiol.236, 2459–2481.
- Alberts, B., Johnson, A., Lewis, J., Morgan, D., Raff, M., Roberts, K., and Walter, P. (2016). Biologia molecolare della cellula, 6th ed. (Zanichelli).
- Ma, Y., Zhang, L., and Huang, X. (2014). Genome modification by CRISPR/Cas9. FEBS J.281, 5186–5193.
- Pinaud, M., and Zamborlini, A. (2025). Electroporation-based CRISPR-Cas9-mediated gene knockout in THP-1 cells and single-cell clone isolation. J. Vis. Exp. (216), e67469.